Available online at www.sciencedirect.com
ScienceDirect
Applied Catalysis B: Environmental 82 (2008) 50–57
APPLIED CATALYSIS B: ENVIRONMENTAL
www.elsevier.com/locate/apcatb

Plasma-assisted catalytic oxidation of methane On the influence of plasma energy deposition and feed composition

Rui Marques [a], Stéphanie Da Costa [b], Patrick Da Costa [a,*]

[a] Université Pierre et Marie Curie, Paris 6, Laboratoire Réactivité de Surface, UMR CNRS 7609, 4 place Jussieu, Case 178 Tour 54-55, 75252 Paris Cedex 05, France

[b] Gaz de France, Direction de la Recherche, 361 av du Président Wilson, B.P. 33, 93211 Saint Denis La plaine Cedex, France

Received 7 November 2007; received in revised form 14 December 2007; accepted 21 December 2007
Available online 17 January 2008

Abstract

The total oxidation of methane was carried out within a dielectric barrier discharge (DBD) reactor. The effect of energy deposition was studied, with energy deposition ranging from 36 to 100 J L^{-1}. In the current study, we also investigated the combined process of a dielectric barrier discharge and γ-alumina catalyst in the total oxidation of methane. In order to separate the catalytic effects from the plasma activation, the work included both purely catalytic and plasma activation processes. It was found that the catalytic activity depended on the energy deposition and the temperature. The plasma process leads to methane conversion in the temperature range of 300–500 °C, whereas, methane conversion was only active above 425 °C when only a catalyst was present. Moreover, the addition of NO_x and CO_2 in the feed was also studied. This addition does not affect the methane conversion in the absence or in the presence of catalyst. Finally, the presence of γ-alumina leads to CO + CO_2 as products of the total oxidation of methane, whereas for the plasma-induced process, CO is the major product of the reaction.

Keywords: Natural gas; Oxidation; Catalysis; Plasma DBD; Alumina

1. Introduction

Catalytic processes for total oxidation of methane have been studied as an alternative to conventional thermal combustion [1–5]. The main application of total catalytic oxidation is the elimination of methane emissions from natural gas decreases the greenhouse gas effect [6]. Today's environmental concerns push governments to diversify energy sources. The huge world-wide presence of natural gas, much larger than crude oil, in addition with the fact that the natural gas combustion offers significant environmental advantages, makes it an attractive alternative to sources such as gasoline and diesel. Although the several advantages of natural gas combustion, the emission of unburned methane (natural gas is typically 90–95% of methane) is a negative point, because methane is a potent greenhouse gas, which is recognised to contribute more to global atmosphere warming than CO_2 at equivalent emission rates, moreover its lifetime is quite long [6]. Methane emissions are now being taken into account in present and future regulations [7]. Therefore, emissions of methane must be necessarily reduced.

Several studies have been performed to design catalytic materials that present the highest activity at the lowest temperature and the best resistance to poisons present in exhaust gases [6,8–15]. The most commonly used catalysts for complete methane oxidation are platinum (Pt) and palladium (Pd) based catalysts. The ratio of CH_4:O_2 in the feed is determined for the catalytic activity of Pt/Al_2O_3 and Pd/Al_2O_3 [9,10]. There are several studies in which the Pd based catalyst and various supports have been tested, such as, alumina, Ta_2O_3, TiO_2, CeO_2 and ZrO_2 [16]. Many fewer studies have been performed concerning Pt catalysts supported on oxides supports compared to Pd catalysts [6]. The future of catalytic oxidation consists of the association of platinum and palladium in bimetallic catalytic systems in order to combine the high activity of Pd catalysts to the high resistance of Pt ones against sulphur poisoning. Recently, rhodium has been also used as promoter on palladium based catalysts [17]. The authors

* Corresponding author. Tel.: +33 1 44 27 36 26; fax: +33 1 44 27 60 33.
E-mail address: dacosta@ccr.jussieu.fr (P. Da Costa).

0926-3373/$ – see front matter © 2008 Elsevier B.V. All rights reserved.
doi:10.1016/j.apcatb.2007.12.024

claimed that cooperation between PdO and Rh_2O_3 seems to explain the higher catalytic performance of bimetallic Pd-Rh catalysts.

In the last years, various thermal and non-thermal plasmas such as dielectric barrier discharge (DBD), corona, gliding arc, microwave, glow discharge and pulsed discharge, have been widely investigated in the field of environment. In plasmas gaseous species are chemical dissociated producing excited species (molecules, atoms) and activated particles (ions, radicals) by electron impact.

Plasmas, non-coupled or coupled with catalysis, are a powerful technology for several applications, such as methane conversion into higher hydrocarbons [17–27], methane reforming [23,28–39] and NO_x reduction [29,40–48]. Alumina was already used as catalyst in plasma catalytic process for acetylene oxidation [49] and for NO_x abatement [54].

Most of the products produced using corona, microwave, and radio frequency discharges are small molecules, such as ethylene, acetylene, hydrogen and carbon monoxide. Complex products including light hydrocarbons, liquid fuels, alcohols and acids are often produced with a DBD [22]. Although the various studies performed, plasma technology was not studied as a way to oxide methane into CO_2 from emissions of combined heat powers (CHP). However, recently, Hueso et al. have used lanthanum substituted Perovskites and silica as catalysts in plasma catalytic process for methane oxidation [46].

This paper presents the results of experiments with a DBD for total methane oxidation. In this study, we determined the influence of temperature and energy deposition in the activity of methane oxidation. Moreover, the influence of CO_2 in the feed was also studied using a typical concentration present in natural gas CHP. The results were compared with those in the absence of CO_2. Finally, the catalytic activity of γ-alumina was tested in the absence and in the presence of plasma DBD.

2. Experimental

A schematic view of the DBD reactor is shown in Fig. 1. The reactor was a quartz tube with an inner diameter of 12 mm a thickness of 2 mm and a length of 500 mm. It has been decomposed in two zones. The plasma was created in the first zone and, in the second one the catalyst could be placed, if necessary.

The electrical discharge reactor is DBD. The reactor geometry was one of wire to cylinder type. It consisted of a tungsten wire (thickness, 0.9 mm) centred in a dielectric tube, and fixed with two ceramic rings. The outer surface of tube was coated with a brass wire to form the outer electrode.

The length of the discharge zone was 150 mm, with a gap of 5.5 mm, resulting in a reaction volume of approximately 14.5 cm^3. To drive the discharge an AC high voltage was generated with a maximum of 14 kV. The high voltage is purchased by GREMI-ESPEO (Orléans). Details of this homemade generator are given in [50]. The applied voltage and current were measured using a high voltage probe (TEKTRONIX P6015A, 1000×) and a current probe (EURO-

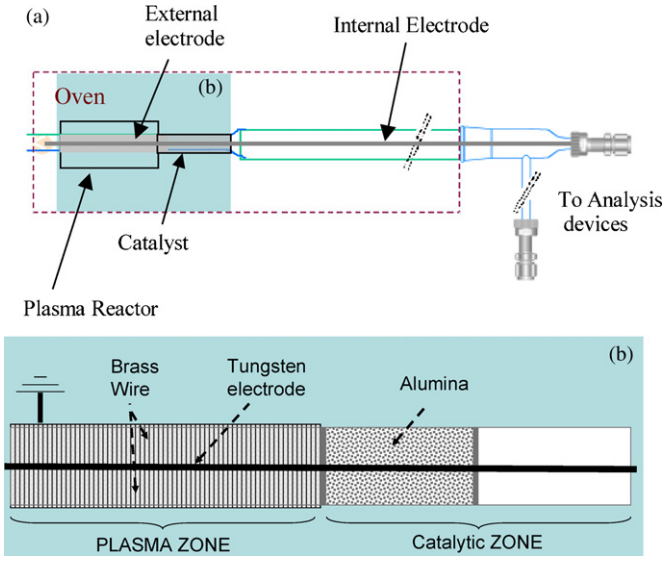

Fig. 1. Dielectric barrier experimental device (a) global scheme, (b) plasma + - catalytic zones.

PULSE 9001), respectively. The output signals were transmitted to a digitizing oscilloscope (TEKTRONIX 2440). The discharge pulse energy into the plasma was measured with a capacitive circuit. The energy deposition in the plasma reactor, J L^{-1} is given by $E_d = (E_p/Q)f$, in which, E_p is the discharge pulse energy, f the pulse repletion frequency, and Q is the gas flow rate at standard conditions (25 °C and 1 atm). In our experimental conditions, the discharge pulse energy E_p was maintained constant at about 15 mJ $pulse^{-1}$. Frequency was varied to obtain the desired energy deposition.

The catalyst in powder form (0.08 mm < Φ < 0.125 mm), surrounded with quartz wool, was placed in the second zone of the reactor, close to the discharge zone (Fig. 1b). The length of the catalytic bed varied from 5 to 20 mm. The bed temperature was measured using a type K thermocouple affixed to the outer reactor surface. The temperature was controlled using an electronic controller (Eurotherm, 2408) and a resistively heated furnace (Eraly). This furnace recovers the plasma and the catalytic zone.

The catalytic activity was measured at atmospheric pressure in the same DBD plasma quartz reactor. Two different reaction mixtures were considered. The reactants are the following: 150 ppm NO, 8% O_2, 7% CO_2, 1000 ppm CH_4 in N_2 as balance which is representative of CHP conditions; and 150 ppm NO, 8% O_2, 0% CO_2, 1000 ppm CH_4 in N_2 as balance, respectively. Furthermore, 150 ppm of NO were chosen in order to reproduce a gas composition close to those observed in exhaust gases of CHP. The NO mixture was supplied by Air Liquide as 0.1% NO, and 99.9% N_2 (<10 ppm other gases). The O_2 mixture contained 100% O_2. The CH_4 mixture contained 1% CH_4, and 99% N_2 (Air Liquide). The CO_2 mixture contained 100% CO_2. The total gas flow was maintained at 0.25 L min^{-1} NTP. Each of the gas mixtures was metered using calibrated electronic mass flow controllers (Brooks, Model 5850E).

The reactor outflow was analyzed using a set of specific detectors. An Eco Physics CLD 700 AL NO_x Chemilumines-

cence analyzer (for NO and total NO_x (*i.e.* NO + NO_2)) allowed the simultaneous detection of NO, NO_2 and NO_x. An Ultramat 6 IR analyzer was used to monitor N_2O and a FID detector was used to follow the total concentration of hydrocarbons (HC). GC–MS analyses were performed on-line using an AGILENT device (GC 6890-MS 5973 N) equipped with a CP-PoraBOND Q capillary column (Chrompack, 30 m long, 0.32 mm inner diameter, 0.5 μm film thicknesses) with temperature programming from 50 to 280 °C. NIST spectral AGILENT data base was used to identify the detected products. The methane concentration was followed by gas micro-chromatography (Agilent G2890A). This apparatus allowed also the analysis of various gases such as H_2, O_2, N_2, CO, and CO_2, in a scale ranging from ppm to %. The analysis time is lower than 120 s.

A commercial γ-Al_2O_3 (Procatalyse) catalyst was used, with specific surface area of 190 $m^2\ g^{-1}$, porous volume 0.7 $cm^3\ g^{-1}$ and grain size 0.80–1.25 mm. In this study, two catalyst weights were considered, 270 and 540 mg, respectively. For 270 mg, the corresponding GHSV is 40,000 h^{-1}, and for 540 mg, the corresponding GHSV is 20,000 h^{-1}.

Steady-state activity, methane conversion, was measured in the presence or in absence of catalyst at different temperatures, ranging from 300 to 500 °C. The methane conversion was defined as follows:

$$\text{methane conversion}\ (\%) = \frac{\text{moles of methane consumed}}{\text{moles of methane introduced}} \times 100$$

For each methane conversion, for example, 10%, the corresponding temperature was denoted T_{10}. These latter temperatures were compared to discuss about the efficiency of plasma conditions or catalytic activity.

3. Results and discussion

3.1. Effect of dielectric material on the methane oxidation

3.1.1. Methane oxidation reaction in absence of CO_2 in the feed

One set of experiments has been carried out without carbon dioxide in the feed. The methane conversion and the NO_x concentration were followed as function of temperature and as function of energy deposition. It is well known that the input power was one of the important parameters in the DBD conversion of methane [23,24,30]. Experiments were conducted in maintaining constant E_p, the discharge pulse energy (14 kV) and Q, the gas flow rate (0.25 L min^{-1}); and in varying f the pulse repletion frequency in the range 10–28 Hz. Then, the energy deposition ranged from 36 to 80 J L^{-1}. The effect of the energy deposition on methane conversion is reported in Fig. 2, as function of temperature. One can see in Fig. 2, that methane is converted from 300 °C in presence of plasma. The effect of energy deposition is not evident at this low temperature. However, at higher temperature, the effect of energy deposition is clearly evident. One can see that at ca. 475 °C, the methane conversion varies from 50% to 80% for energy deposition of 36 and 80 J L^{-1}. Table 1 also indicates that the conversion in methane increases with the energy deposition. Indeed, for 30% methane conversion, the reported temperature, T_{30}, is lower with the energy deposition increasing. All these results might be explained by more active species generated at higher energy deposition.

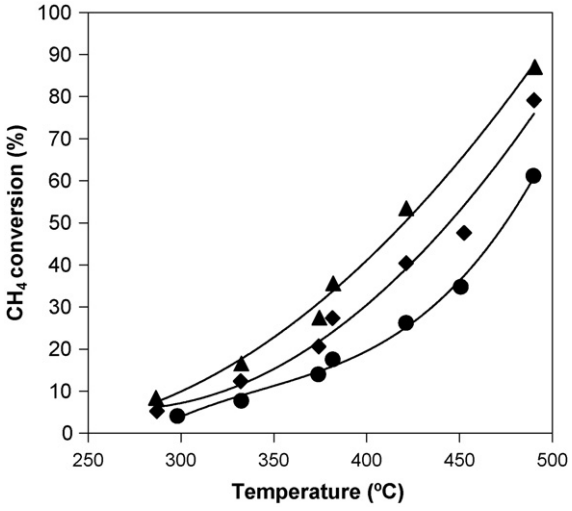

Fig. 2. Effect of energy deposition (J L^{-1}) on the CH_4 conversion as function of temperature (●: 36 J L^{-1}, ◆: 58 J L^{-1} and ▲: 80 J L^{-1}).

From Fig. 2 and Table 1, one can conclude that higher methane conversion is obtained for an energy deposition of 80 J L^{-1} and for temperatures close to 500 °C. However, as reported in Fig. 3, at these temperatures, a large NO_x formation is observed. The NO_x concentration remained constant above 400 °C. However, at higher temperature and depending on the energy deposition, the NO_x concentration reaches 210 ppm (E_d = 80 J L^{-1}), which represents 40% more than the initial concentration in the feed.

In Fig. 4, the NO_x concentration (NO_2 and NO) is presented for an energy deposition of 58 J L^{-1}, as function of temperature. It was found that for 58 J L^{-1}, NO is oxidized to NO_2 in presence of plasma. These results are in agreement with those of Penetrante et al. [51,52,54] and Hoard and Lou Balmer [53].

However, in our experimental condition at high temperature, an excess of NO_x is observed, such as example 200 ppm at 490 °C for an energy deposition of 58 J L^{-1}. This NO_x excess is

Table 1
Temperature of n% methane conversion, (T_n), under different energy deposition, in absence of catalyst for: (a) 150 ppm NO, 8% O_2, 0% CO_2, 1000 ppm CH_4 in N_2 as balance, (b) 150 ppm NO, 8% O_2, 7% CO_2, 1000 ppm CH_4 in N_2 as balance

Energy deposition (J L^{-1})	n% Methane conversion temperature (T_n for n% of conversion) (°C)							
	T_{10}		T_{30}		T_{50}		T_{80}	
	(a)	(b)	(a)	(b)	(a)	(b)	(a)	(b)
36	340	348	435	430	475	470	–	–
58	320	330	400	410	445	450	–	–
80	300	315	375	385	420	430	478	480
100	–	–	–	360	–	403	–	460

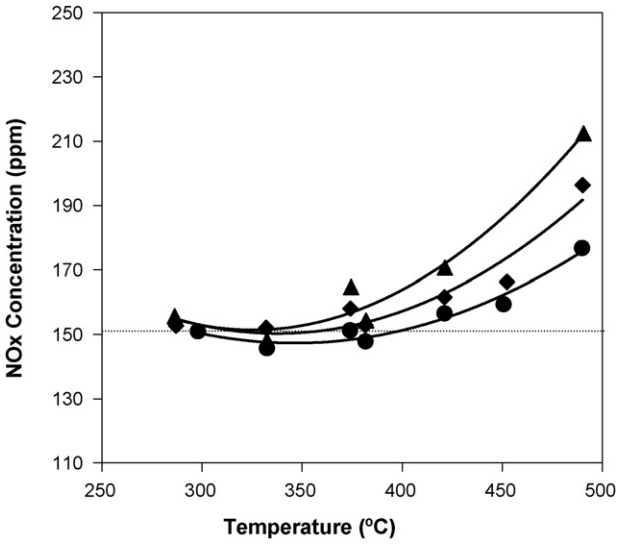

Fig. 3. Effect of energy deposition (J L^{-1}) on NO_x concentration as function of temperature (●: 36 J L^{-1}, ◆: 58 J L^{-1}, ▲: 80 J L^{-1}); 150 ppm NO, 8% O_2, 0% CO_2, 1000 ppm CH_4 in N_2 as balance.

due to NO formation from $N_2 + O_2$ present in excess in the feed. Furthermore, the NO_2 formation is explained by the NO reaction with O_2 in presence of DBD. These latter phenomena have already been described in the literature [42,53,54], for the plasma assisted catalytic reduction of NO_x.

Considering these latter results, the best conversion is obtained for a high methane conversion at high temperature. In order to minimize the NO_x formation a low energy deposition, such as, $E_d = 36$ J L^{-1}should be used.

3.1.2. Methane oxidation reaction in presence of 7 vol.% CO_2 in the feed

The effect of the feed composition was studied by varying the feed CH_4:CO_2 ratio. The used ratio is 1:70 and corresponds

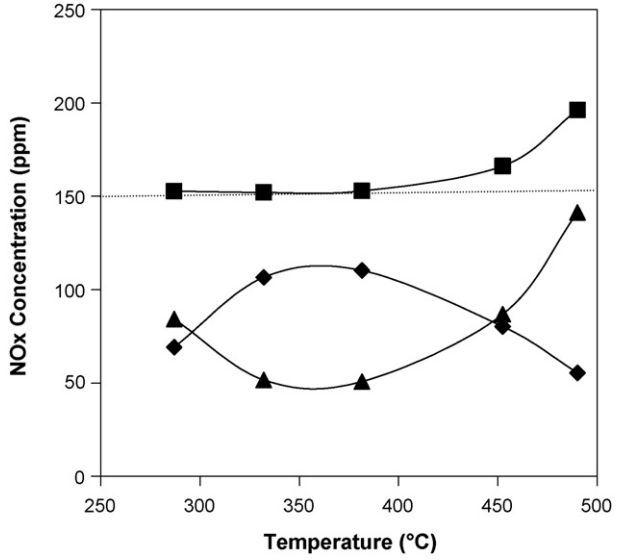

Fig. 4. (▲) NO, (◆) NO_2 and (■) NO_x concentration as function of temperature for an energy deposition of 58 J L^{-1}, in presence of 150 ppm NO, 8% O_2, 0% CO_2, 1000 ppm CH_4 in N_2 as balance.

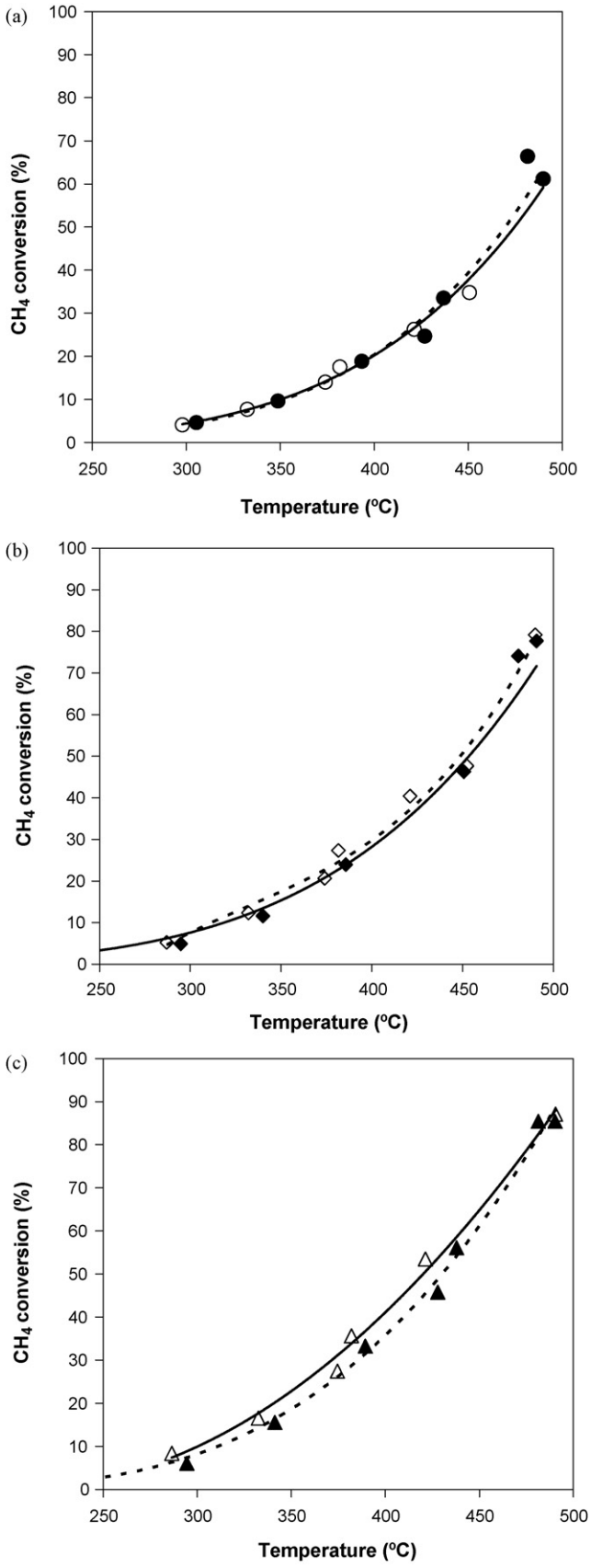

Fig. 5. Effect of CO_2 concentration in the feed on the CH_4 conversion (black symbols) with CO_2 and (white symbols △) without CO_2. (a) Energy deposition = 36 J L^{-1}. (b) Energy deposition = 58 J L^{-1}. (c) Energy deposition = 80 J L^{-1}.

to a significant CH_4:CO_2 ratio of combine heat power (CHP). Table 1 and Fig. 5 present the effect of the energy deposition on the steady-state methane conversion as function of temperature, for CH_4:CO_2 = 1:70. In presence of CO_2 in the feed, the methane conversion increases with the energy deposition. Indeed, in Table 1(b), 50% of methane is converted at 470, 450, 430 °C for E_d = 36, 58, 80 J L^{-1} respectively. In comparison, in absence of CO_2, 50% conversion was obtained at 475, 440, 420 for E_d = 36, 58, 80 J L^{-1} respectively (Table 1(a)). These results indicate that the effect of CO_2 in the feed is not significant for the studied ratio CH_4:CO_2 (Fig. 5). However, in other studies dealing with the methane to acetylene and to syngas, Kado et al. [34] had shown that the presence of CO_2 in the feed, affected the methane conversion in decreasing the C_2 selectivity. In our experimental conditions, only CO and CO_2 were detected.

The effect of NO was also investigated in the presence of CO_2 in the feed. The results are presented in Fig. 6. The NO_x concentration increased with increasing the temperature and the energy deposition. Above 400 °C, NO_x were formed. Indeed, about 10 ppm of NO_x were formed with an E_d = 36 J L^{-1}, at 450 °C. These results are in agreement with those found in absence of CO_2 in the feed (Figs. 3 and 4), in which at 440 °C, about 8 ppm of NO_x were formed. Then, the presence of CO_2 does not affect the NO_x formation at high temperature. Again, the best gas treatment process is obtained for high methane conversion in minimizing the NO_x formation, at high temperature (>400 °C), and using an energy deposition E_d = 36 J L^{-1}.

3.2. Catalytic performance

In absence of plasma, the γ-alumina was active only at 415 °C and above leading to CO_2 and H_2O. The catalytic performance alone is presented in Fig. 7, for two different space velocities, GHSV = 20,000 and 40,000 h^{-1} respectively. The methane conversion over γ-alumina alone was about 8% and 2% for GHSV = 20,000 and 40,000 h^{-1} respectively at 450 °C and about 30% and 12% for GHSV = 20,000 and 40,000 h^{-1} respectively at 475 °C. Then, it was shown that the activity in presence of γ-alumina was very poor. However, in absence of plasma, no NO_x formation was observed at high temperature. Therefore, we can expect that the combination of plasma and alumina leads to less NO_x formation at high temperature [51].

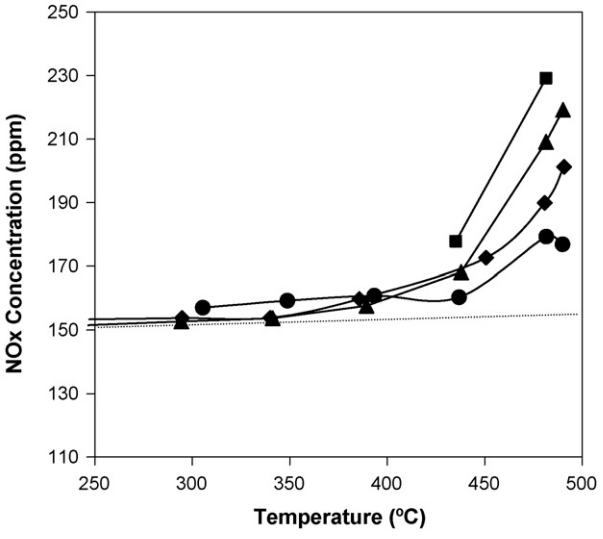

Fig. 6. Effect of energy deposition (J L^{-1}) on NO_x concentration as function of temperature (●: 36 J L^{-1}, ◆: 58 J L^{-1}, ▲: 80 J L^{-1} and ■: 100 J L^{-1}); 150 ppm NO, 8% O_2, 7% CO_2, 1000 ppm CH_4 in N_2 as balance.

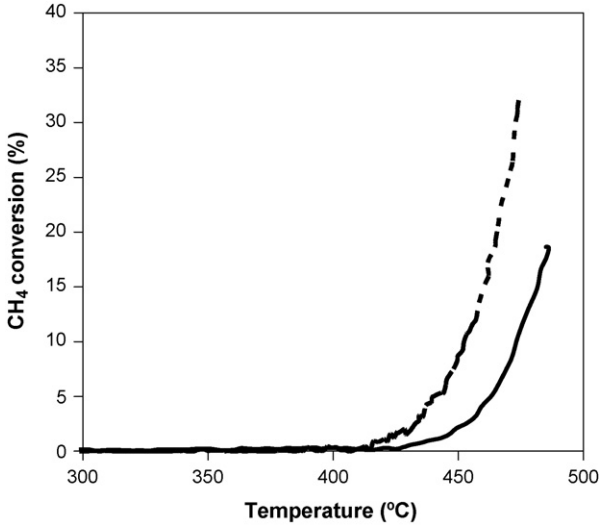

Fig. 7. Effect of γ-Al_2O_3 on CH_4 conversion as function of the temperature: (GHSV = 20,000 h^{-1}, 540 mg) (- - - - - - -); (GHSV = 40,000 h^{-1}, 270 mg) (—).

3.3. Plasma catalytic oxidation of methane

Alumina catalyst was placed after the discharge zone of plasma to improve the selectivity and the efficiency of plasma process.

Our motivation is based on other plasma-catalytic applications such as methane valorization [25,27,29] and NO_x emission remediation [42,53,54], in which is well known that the combination of plasma and catalysis leads to a better activity and a better selectivity than both catalysis and plasma alone [42,54].

We have shown that the alumina alone is only active at high temperature (Fig. 7). Indeed, the catalytic methane activation is very difficult to perform. Only noble metal catalysts lead to methane conversion at low temperature (<300 °C) [6]. However, in presence of plasma, one part of methane is already activated.

Park et al. [55] had proposed some reactions induced by the plasma on CH_4 in presence of O_2 and NO in the feed:

$$CH_4 + O \rightarrow CH_3 + OH \quad (1)$$

$$CH_3 + O_2 + M \rightarrow CH_3O_2 + M \quad (2)$$

$$CH_3O_2 + NO \rightarrow CH_3O + NO_2 \quad (3)$$

$$CH_3 + CO \rightarrow CH_3CO \quad (4)$$

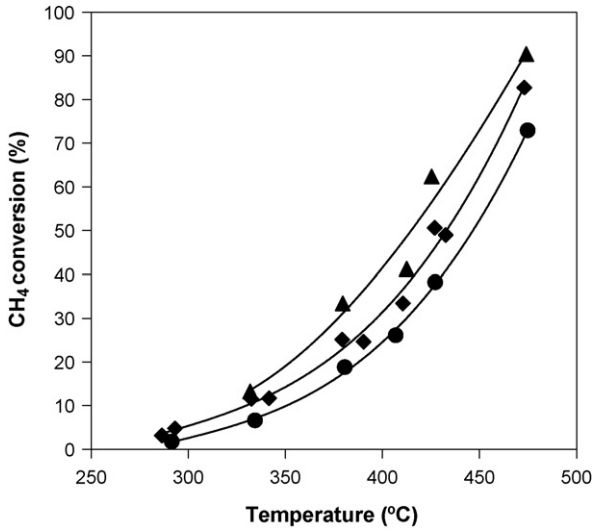

Fig. 8. Effect of energy deposition (J L^{-1}) on the CH_4 conversion as function of temperature (●: 36 J L^{-1}, ◆: 58 J L^{-1}, and ▲: 80 J L^{-1}), over γ-Al_2O_3 (GHSV = 20,000 h^{-1}, 540 mg) 150 ppm NO, 8% O_2, 7% CO_2, 1000 ppm CH_4 in N_2 as balance.

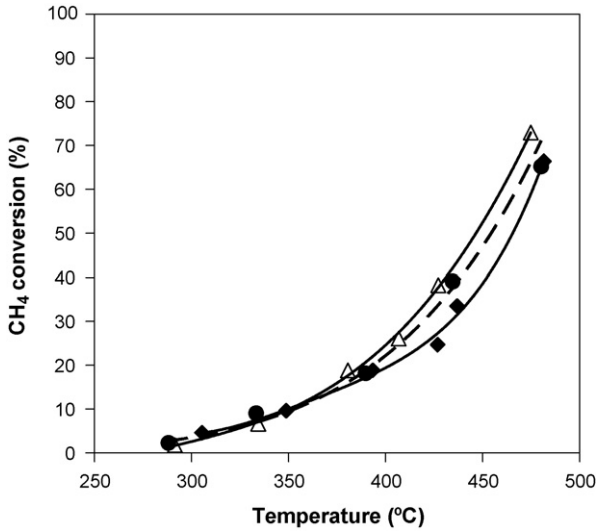

Fig. 9. CH_4 conversion as function of temperature in absence or in presence of γ-Al_2O_3, for an energy deposition equal to 36 J L^{-1} (◆ in absence of catalyst, ● in presence of γ-Al_2O_3 (GHSV = 40,000 h^{-1}, 270 mg)), (Δγ-Al_2O_3 (GHSV = 20,000 h^{-1}, 540 mg)); 150 ppm NO, 8% O_2, 7% CO_2, 1000 ppm CH_4 in N_2 as balance).

The activated species such as CH_3, CH_3O_2 and CH_3CO are more reactive than the methane.

The methane conversion was followed as function of temperature and as function of energy deposition, in presence of plasma + alumina. As reported in Fig. 8, the effect of energy deposition on methane conversion is only evident at high temperature for a plasma catalytic system. Table 2 also indicates that the methane conversion increases with the energy deposition, in presence of plasma + alumina. The temperature found for 50% methane conversion decreases with increasing E_d. In Table 2, 50% conversion is obtained at 448, 435 and 415 °C for E_d = 36, 58 and 80 J L^{-1} respectively. These results are in agreement with those presented in Table 1, obtained in absence of alumina. For a fixed energy deposition, the presence of alumina leads to decrease the temperature for a fixed conversion (X%) of about 10–20 °C. Moreover, 80% conversion is only obtained in presence of plasma + alumina, at 470 °C for E_d = 58 J L^{-1}. For the same E_d, in absence of catalyst, 80% conversion was not obtained in the range of the studied temperature (300–500 °C). This better activity in presence of plasma + alumina could be explained by the better reactivity of the activated species, induced by the plasma. In fact, the plasma created reactive species from methane, and then these species reacted with the catalyst leading to higher methane conversion.

The effect of space velocity (GHSV), corresponding to alumina was also studied. The weight of alumina was changed to obtain a GHSV = 40,000 h^{-1}. The corresponding results are reported in Fig. 9. A comparison with a lower space velocity was also presented. For a fixed energy deposition, the methane conversion obtained, in the range of studied temperatures are very close, for the two experimental conditions. Indeed, for a GHSV = 40,000 h^{-1}, the conversion was 39% at 440 °C, whereas for a GHSV = 20,000 h^{-1}, the conversion was 38% at 435 °C. Therefore, the effect of space velocity is negligible. The plasma has created species that reacted with alumina leading to CO_2 and H_2O. With the lower amount of alumina, which corresponds to GHSV = 40,000 h^{-1}, the reactive species created from CH_4, have already reacted totally with alumina to form to CO, CO_2 and H_2O. Then, it is not necessary to increase the amount of alumina. Indeed, by decreasing the GHSV = 20,000 h^{-1}, similar methane conversion were obtained (Fig. 9).

The selectivity in CO was also studied in absence and in presence of alumina (Fig. 10a and b). The CO_2 concentration was not detected due to the presence of CO_2 in the feed. In

Table 2
Temperature of n% methane conversion, (T_n), under different energy deposition, in presence of catalyst (GHSV = 20,000 h^{-1}, 540 mg), comparison with temperature of n% methane conversion, (T_n), under different plasma discharges, in absence of catalyst (150 ppm NO, 8% O_2, 7% CO_2, 1000 ppm CH_4 in N_2 as balance)

Energy deposition (J L^{-1})	n% Methane conversion temperature (T_n for n% of conversion) (°C)					
	T_{30}		T_{50}		T_{80}	
	Plasma alone	Plasma and Al_2O_3	Plasma alone	Plasma and Al_2O_3	Plasma alone	Plasma and Al_2O_3
36	430	412	470	448	–	–
58	410	398	450	435	–	470
80	385	377	430	415	480	460

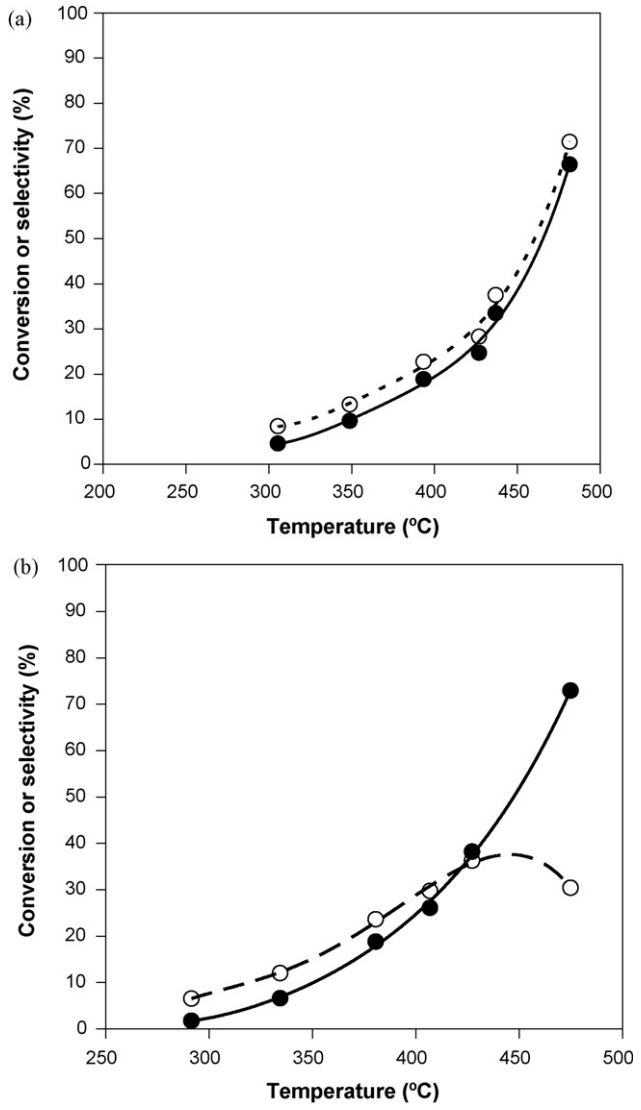

Fig. 10. CH_4 (●) conversion and CO (○) selectivity as function of the temperature for an energy deposition of 36 J L^{-1}, 150 ppm NO, 8% O_2, 7% CO_2, 1000 ppm CH_4 in N_2 as balance; (a) in absence of γ-Al_2O_3; (b) over γ-Al_2O_3 (GHSV = 20,000 h^{-1}, 540 mg).

presence of plasma, the CO_2 leads to CO formation in the range of working temperature. In fact, experiments were performed in presence of plasma and in absence of catalyst, in flowing 150 ppm NO, 8% O_2, 7% CO_2, 1000 ppm CH_4 in N_2 as balance. The CO formation is then slightly higher than the methane conversion (Fig. 10a). Therefore, CO_2 led to CO + O in presence of $E_d = 36$ J L^{-1}. In presence of catalyst, at temperature higher than 425 °C, the CO formation was lower than methane conversion (Fig. 10b). This latter result can be explained by the CO oxidation in CO_2 over alumina. Finally, the combination of plasma and alumina led to a higher activity for methane total oxidation than alumina or plasma used alone.

4. Conclusions

The methane total oxidation was studied as function of temperature, by changing the energy deposition (E_d). At low energy deposition, $E_d = 36$ J L^{-1}, methane was converted at 300 °C and above. The methane conversion increased with increasing the energy deposition. However, for high temperatures, then for the high methane oxidation efficiency, NO_x were formed during the plasma process. Therefore, to minimize NO_x formation and to obtain the highest methane conversion led us to carry out experiments at temperatures around 400 °C, but in presence of low energy deposition, $E_d = 36$ J L^{-1}.

In industrial conditions, CO_2 is present in a large excess in the feed., The effect of CO_2 was then studied. The used CH_4:CO_2 ratio is 1:70 and corresponds to a significant CH_4:CO_2 ratio of combine heat power (CHP). No effect of CO_2 was observed on the methane conversion. However, in absence of catalyst in the plasma system, CO was formed from the CO_2 decomposition ($CO_2 \rightarrow CO + O$).

The alumina alone, used as catalyst, was active at 425 °C and above. The activity of this catalyst is then very poor. However, no NO_x were formed in absence of plasma with the catalytic system alone.

Finally, the plasma catalytic oxidation of methane was studied in presence of alumina. For the same energy deposition, the methane oxidation is favored in presence of plasma + alumina system, in comparison to plasma or alumina alone. This better activity in presence of plasma + alumina could be explained by the better reactivity of the activated species, induced by the plasma. In fact, the plasma created reactive species from methane, and then these species reacted with the catalyst, placed after the discharge, leading to higher methane conversion. However, the effect of the weight of catalyst is not evident. Two different space velocities have been used (GHSV = 20,000 h^{-1} and 40,000 h^{-1}), but similar conversions have been calculated.

Finally, the selectivity in CO_2 and CO was followed for the different experimental conditions. In presence of catalyst, at temperature higher than 425 °C, the CO formation was lower than methane conversion, where as in absence of catalyst the CO formation was always higher than the methane conversion. These latter results can be explained by the CO oxidation in CO_2 over alumina, where as in the presence of plasma alone, CO is not treated.

We can conclude that combination of plasma and alumina led to a higher activity for methane total oxidation than alumina or plasma used alone. However, the temperatures of total oxidation remain very high. To decrease the temperature reaction, the alumina catalyst, which had not presented a high activity, could be replaced by a typical methane oxidation catalyst, such as a supported-platinum or a supported-palladium based catalyst [6]. In a future paper, we will present the effect of palladium or platinum in the plasma catalytic total oxidation of methane.

Acknowledgements

The authors thank Gaz de France for the financial support and Dr. A. Khacef, from Laboratory of GREMI (Orleans) for purchasing the High Voltage device.

References

[1] D.L. Trimm, Appl. Catal. 7 (1983) 249.
[2] R. Prasad, L.A. Kennedy, E. Ruckenstein, Catal. Rev. Sci. Eng. 26 (1984) 1.
[3] L.D. Pfefferle, W.C. Pfefferle, Catal. Rev. Sci. Eng. 29 (1987) 219.
[4] Z.R. Ismagilov, M.A. Kerzhenzev, Catal. Rev. Sci. Eng. 32 (1990) 51.
[5] M.F.M. Zwinkels, S.G. Järås, P.G. Menon, T.A. Griffin, Catal. Rev. Sci. Eng. 35 (1993) 319.
[6] P. Gélin, M. Primet, Appl. Catal. B 39 (2002) 1.
[7] A.A.L. Barry, M.M. Van Setten, J.A. Moulijn, Catal. Rev. 43 (2001).
[8] S.E. Oh, P.J. Mitchell, R.M. Siewert, J. Catal. 132 (1991) 287.
[9] R. Burch, P.K. Loader, Appl. Catal. B 5 (1994) 149.
[10] C.F. Cullis, B.M. Willatt, J. Catal. 83 (1983) 267.
[11] M. Niwa, K. Awano, Y. Murakami, Appl. Catal. 7 (1983) 317.
[12] K. Muto, N. Katada, M. Niwa, Appl. Catal. A 134 (1996) 203.
[13] L. Ma, D.L. Trimm, C. Jiang, Appl. Catal. A 138 (1996) 275.
[14] A.F. Ahlström-Silversand, C.U.I. Odenbrand, Appl. Catal. A 153 (1997) 157.
[15] J.C. Van Giezen, F.R. van den Berg, J.L. Kleinen, A.J. van Dillen, J.W. Geus, Catal. Today 47 (1999) 287.
[16] R.J. Farrauto, J.K. Lampert, M.C. Hobson, E.M. Waterman, Appl. Catal. B 62 (1995) 63.
[17] A. Maione, F. André, P. Ruiz, Appl. Catal. A 333 (2007) 1.
[18] J.H. Lunsford, Catal. Today 63 (2000) 165.
[19] J.M. Fox, Catal. Rev. Sci. Eng. 35 (1993) 169.
[20] Ch. Liu, A. Marafee, R.G. Mallinson, L. Lobban, Appl. Catal. 164 (1997) 21.
[21] M. Okumoto, A. Mizuno, Catal. Today 71 (2001) 11.
[22] S.-S. Kim, L. Hwaung, B.-K. Na, H.K. Song, Catal. Today 89 (2004) 193.
[23] Y.-P. Zhang, Y. Li, Y. Wang, C.-J. Liu, B. Eliasson, Fuel Proc. Technol. 83 (2003) 101.
[24] T. Jiang, Y. Li, C.-J. Liu, G. Xu, B. Eliasson, B. Xue, Catal. Today 72 (2002) 229.
[25] M. Heintze, M. Magureanu, J. Catal. 206 (2002) 91.
[26] W. Cho, Y. Baek, S.-K. Moon, Y.C. Kim, Catal. Today 74 (2002) 207.
[27] X. Zhang, B. Dai, A. Zhu, W. Gong, C. Liu, Catal. Today 72 (2002) 223.
[28] C.-J. Liu, R. Mallison, L. Lobban, Appl. Catal. A 178 (1999) 17.
[29] M. Heintze, B. Pietruszka, Catal. Today 89 (2004) 21.
[30] B. Pietruszka, K. Anklam, M. Heintze, Appl. Catal. A 261 (2004) 19.
[31] H.K. Song, J.W. Choi, S.H. Yue, H. Lee, B.K. Na, Catal. Today 89 (2004) 27.
[32] M. Kraus, B. Eliasson, U. Kogelschatz, A. Wokam, P.C.C.P. 3 (2001) 294.
[33] M.W. Li, G.H. Xu, Y.L. Tian, L. Chen, H.F. Fu, J. Phys. Chem. 108 (2004) 1687.
[34] S. Kado, K. Urasaki, Y. Sekine, K. Fujimoto, Fuel 82 (2003) 1377.
[35] S.L. Yao, A. Nakayama, E. Suzuki, Energy Fuels 15 (2001) 1295.
[36] A. Czernichowski, Oil Gas Sci. Technol. Rev. IFP 56 (2001) 181.
[37] L. Bromberg, D.R. Cohn, A. Rabinovich, C. O'Brien, S. Hochgreb, Energy Fuels 12 (1998) 11.
[38] S.L. Yao, F. Ouyang, A. Nakayama, E. Suzuki, M. Okumoto, A. Mizuno, AIChE Spring Meeting, Atlanta, GA, 2000.
[39] S.L. Yao, F. Ouyang, A. Nakayama, E. Suzuki, M. Okumoto, A. Mizuno, Energy Fuels 14 (2000) 910.
[40] S.L. Yao, A. Nakayama, E. Suzuki, AIChE J. 47 (2001) 413.
[41] Th. Hammer, Th. Kappes, M. Baldauf, Catal. Today 89 (2004) 5.
[42] O. Gorce, H. Jurado, C. Thomas, G. Djéga-Mariadassou, A. Khacef, J.M. Cormier, J.M. Pouvesle, G. Blanchard, S. Calvo, Y. Lendresse, SAE Technical Paper Series 2001-01-3508 (2001).
[43] K.P. Francke, H. Miessner, R. Rudolph, Catal. Today 59 (2000) 411.
[44] A. Khacef, J.M. Cormier, J.M. Pouvesle, J. Phys. D Appl. Phys. 35 (2002) 1491.
[45] H. Lin, X. Gao, Z. Luo, K. Cen, Z. Huang, Fuel 83 (2004) 1349.
[46] J.L. Hueso, A. Caballero, J. Cotrino, A.R. Gonzalez-Elipe, Catal. Commun. 8 (2007) 1739.
[47] M. Magureanu, V.I. Parvulescu, in: P. Granger, V.I. Parvulescu (Eds.), Studies in Surface Science, vol. 171, Elsevier, 2007, p. 361.
[48] J.L. Hueso, J. Cotrino, A. Caballero, J.P. Espinos, A.R. Gonzalez-Elipe, J. Catal. 247 (2007) 288.
[49] A. Rousseau, A.V. Meshchanov, J. Roepcke, Appl. Phys. Lett. 88 (2006) 021503.
[50] A. Khacef, R. Viladrosa, C. Cachonciville, E. Robert, J.M. Pouvesle, Rev. Sci. Instrum. 78 (1997) 2292.
[51] B.M. Penetrante, in: B.M. Penentrante, S.E. Schultheis (Eds.), Non-thermal Plasma Technique for Pollution Control—Part A: Overview, Fundamentals and Supporting Technologies, Springer Verlag, Berlin/Heidelberg/New York, 1993, p. 65.
[52] B.M. Penetrante, J.N. Bardsley, M.C. Hsiao, Jpn. J. Appl. Phys. 36 (1997) 5007.
[53] J. Hoard, M. Lou Balmer, SAE Technical Paper Series 982429 (1998).
[54] B.M. Penetrante, R.M. Brusasco, B.T. Meritt, W.J. Pitz, G.E. Volgtlin, M.C. Kung, H.H. Kung, C.Z. Won, K.E. Voss, SAE Technical Paper Series 982508 (1998).
[55] K.S. Park, D.I. Kim, H.S. Lee, K.M. Chun, B.H. Chun, SAE Technical Paper Series 2001-01-3515 (2001).